Supporting Information

Pick et al. 10.1073/pnas.1215142110

SI Materials and Methods

Metabolite Extraction. For metabolite analysis, 100 mg (fresh weight) of powdered tissue was extracted with 700uL of methanol for 15 min at 70 °C. Then, 700 uL of water and 375 uL of chloroform were added, and the samples were incubated in a rotating shaker for 30 min at 4 °C (modified after ref. 1). The phases were separated, and the methanol/water phase was retained for further experiments. Amino acid contents were determined directly from the extract exactly as described in ref. 2, except that the samples were extracted in 1:1 (vol/vol) methanol/water. Polar metabolites were analyzed as described (1). Briefly, 50 uL of the extract was dried in a speed-vac, and carbonyl moieties were protected by methoximation using a 20 mg/mL solution of methoxyamine hydrochloride in pyridine at 30 °C for 90 min. Acidic protons were modified with *N*-methyl-*N*-trimethylsilyltrifluoroacetamide at 37 °C for 30 min. Samples were injected at 230 °C, separated on HP5 columns for 30 min, and analyzed from m/z = 50 to m/z = 800 in total ion scans in an Agilent Technologies 5973 inert mass spectrometer. Metabolites were identified by comparison with the retention time and the fractionation pattern of standards and quantified with external standard curves of complex standards. The complex standard for liquid chromatography/MS contained all amino acids. The complex standard for GC/MS contained glucose, fructose, glycolate, succinate, glycerate, fumarate, malate, 2-oxoglutarate, citrate, isocitrate, myo-inositol, sucrose, glycine, serine, pyruvate, maltose, and ribitol at concentrations of 0.1, 0.5, 1, 5, 10, 50, and 100 μM. The complex standard was injected before the randomized samples, after injection of 21 samples and at the end of the measurement. Retention times and peak size for the complex standards remained stable.

Metabolite Extraction Optimized for Photorespiratory Metabolites. The extraction procedure was conducted at 4 °C. Fifty milligrams of powdered material was extracted with 600 μL of ice-cold *N*,*N*-dimethiylformamide. Following the addition of 400 μL of water, the samples were shaken for 10 min and separated into phases by centrifugation for 8 min at 22,00 × *g*. The upper aqueous phase was mixed with 600 μL of xylene for 10 min and centrifuged for 3 min. Upper organic phase was discarded, and 300 μL of lower aqueous phase was dried for the analysis. The GC/MS analysis was conducted exactly as described by Lisec et al. (3). Chromatograms and mass spectra were evaluated by Chroma TOF 1.6 (Leco) and TagFinder 4.0 (4) for the quantification and annotation of the peaks. The ^{18}O enrichment was calculated according to Berry et al. (5).

1. Fiehn O, Kopka J, Trethewey RN, Willmitzer L (2000) Identification of uncommon plant metabolites based on calculation of elemental compositions using gas chromatography and quadrupole mass spectrometry. *Anal Chem* 72(15):3573–3580.
2. Lu Y, et al. (2008) New connections across pathways and cellular processes: Industrialized mutant screening reveals novel associations between diverse phenotypes in Arabidopsis. *Plant Physiol* 146(4):1482–1500.
3. Lisec J, Schauer N, Kopka J, Willmitzer L, Fernie AR (2006) Gas chromatography mass spectrometry-based metabolite profiling in plants. *Nat Protoc* 1(1):387–396.
4. Luedemann A, Strassburg K, Erban A, Kopka J (2008) TagFinder for the quantitative analysis of gas chromatography—mass spectrometry (GC-MS)-based metabolite profiling experiments. *Bioinformatics* 24(5):732–737.
5. Berry JA, Osmond CB, Lorimer GH (1978) Fixation of 1802 during photorespiration. *Plant Physiol* 62:954–967.

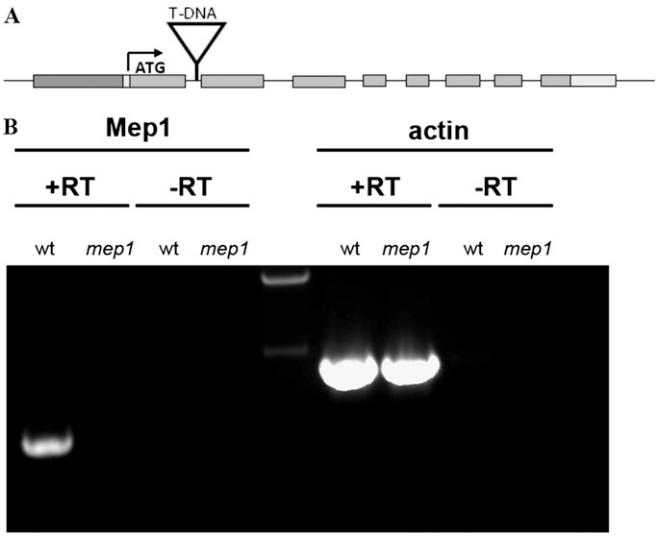

Fig. S1. T-DNA insertion leads to full KO of the gene At1g32080. (*A*) The T-DNA is inserted in the first intron of the gene At1g32080. The arrow symbolizes the transcription start site. Gray boxes stand for exons, lines for introns, dark gray boxes for 5′ UTR, and light gray boxes for 3′ UTR. (*B*) Expression control of the KO gene. WT and mutant gene show actin expression. Only WT shows PLGG1 expression.

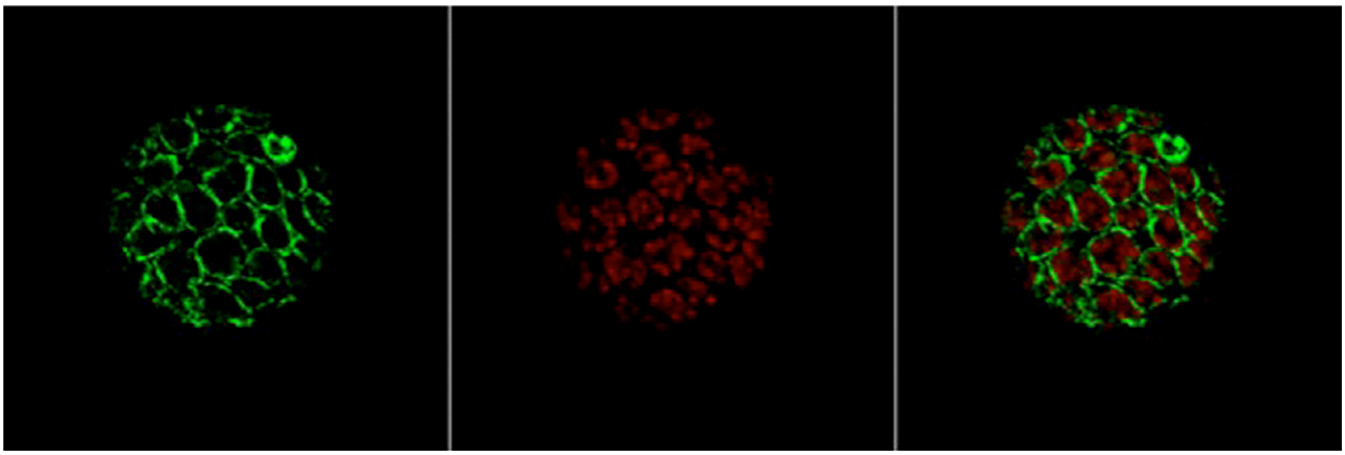

Fig. S2. PLGG1 is located at the chloroplast envelope. GFP fluorescence (*Left*), chlorophyll autofluorescence (*Center*), and merge of both signals (*Right*). GFP was fused C-terminal translationally to the full-length PLGG1 protein. The construct was transiently expressed in *Nicotiana benthaminana*. Protoplasts were used for microscopic detection of the GFP signal.

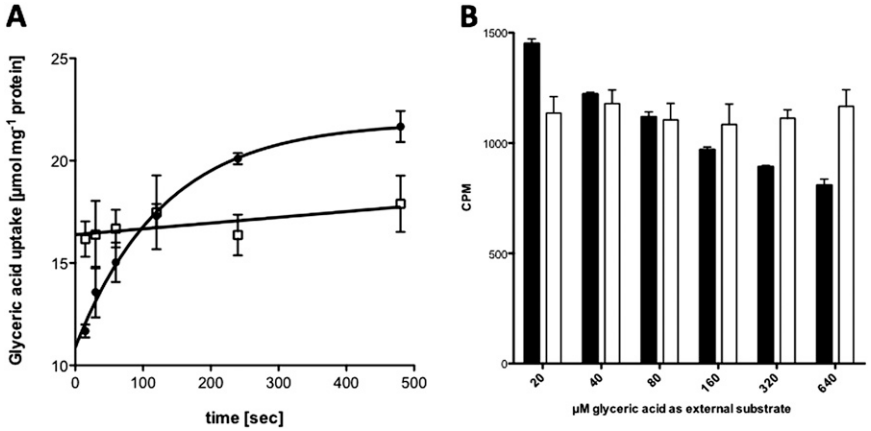

Fig. S3. PLGG1 shows an active and time-dependent uptake of [^{14}C]Glycerate that can be inhibited by increasing concentrations of unlabeled glycerate. (*A*) Time-dependent uptake of radiolabeled [^{14}C]Glycerate (50 μM external concentration) in the presence (●) or absence (□) of glycolate as internal substrate (20 mM). In the presence of a suitable counterexchange substrate inside the liposomes (e.g., glycolate) a Michaelis–Menten-type saturation kinetics was observed. In control liposomes preloaded with equal amounts of buffer or in liposomes that did not contain reconstituted PLGG1, only unspecific diffusion of the labeled substrate was observed. (*B*) Concentration-dependent inhibition of active transport in the presence (filled bars) or absence of glycolate (open bars) as internal substrate (20 mM). Active transport was inhibited with increasing external glycerate concentrations, whereas passive diffusion was independent on external glycerate concentration. Error bars represent SD of three independent uptake experiments. Recombinant At1g32080 protein was expressed in vitro by using the 5PRIME wheat germ expression kit as described (1) and reconstituted into liposomes by using reconstitution and uptake buffers as described in Howitz et al. (2).

1. Nozawa A, et al. (2007) A cell-free translation and proteoliposome reconstitution system for functional analysis of plant solute transporters. *Plant Cell Physiol* 48(12):1815–1820.
2. Howitz KT, McCarty RE (1991) Solubilization, partial purification, and reconstitution of the glycolate/glycerate transporter from chloroplast inner envelope membranes. *Plant Physiol* 96(4):1060–1069.

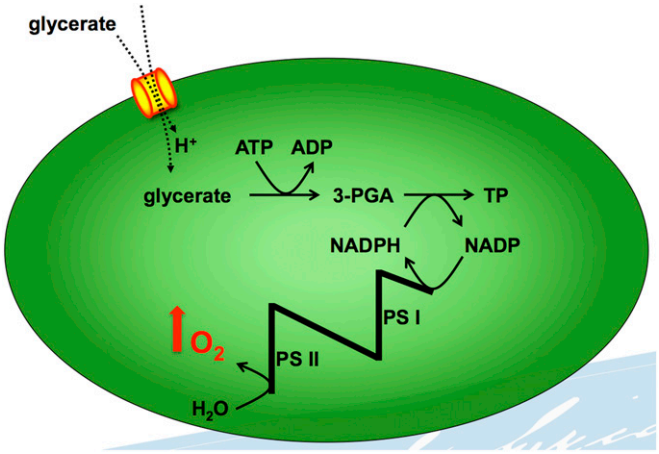

Fig. S4. Scheme of glycerate-dependent oxygen evolution. Glycerate is transported by PLGG1 into the chloroplast in a proton-dependent manner and converted to 3-PGA under ATP consumption. 3-PGA is converted to triose phosphates (TP) under NADPH consumption. NADP is regenerated to NADPH at the photosynthetic electron transport chain under water consumption and oxygen evolution (red arrow).

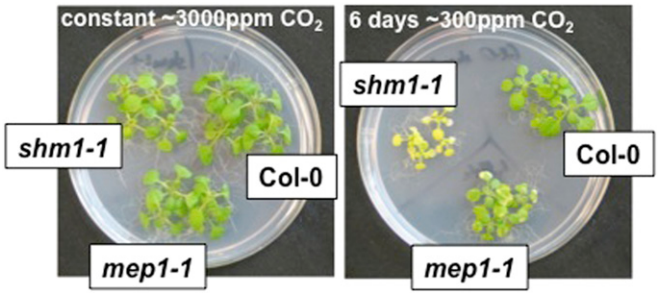

Fig. S5. Photorespiratory phenotype of *plgg1-1* seedlings. Seedlings were from *A. thaliana* Col-0 (WT), the photorespiratory mutant *shm1-1* (impaired in mitochondrial SHMT), and the T-DNA insertion line *plgg1-1*. Plants were grown on MS medium under elevated CO_2 concentrations (3,000 ppm) for 10 d (*Left*) or for 4 d and shifted to ambient CO_2 (300 ppm) for 6 d (*Right*).

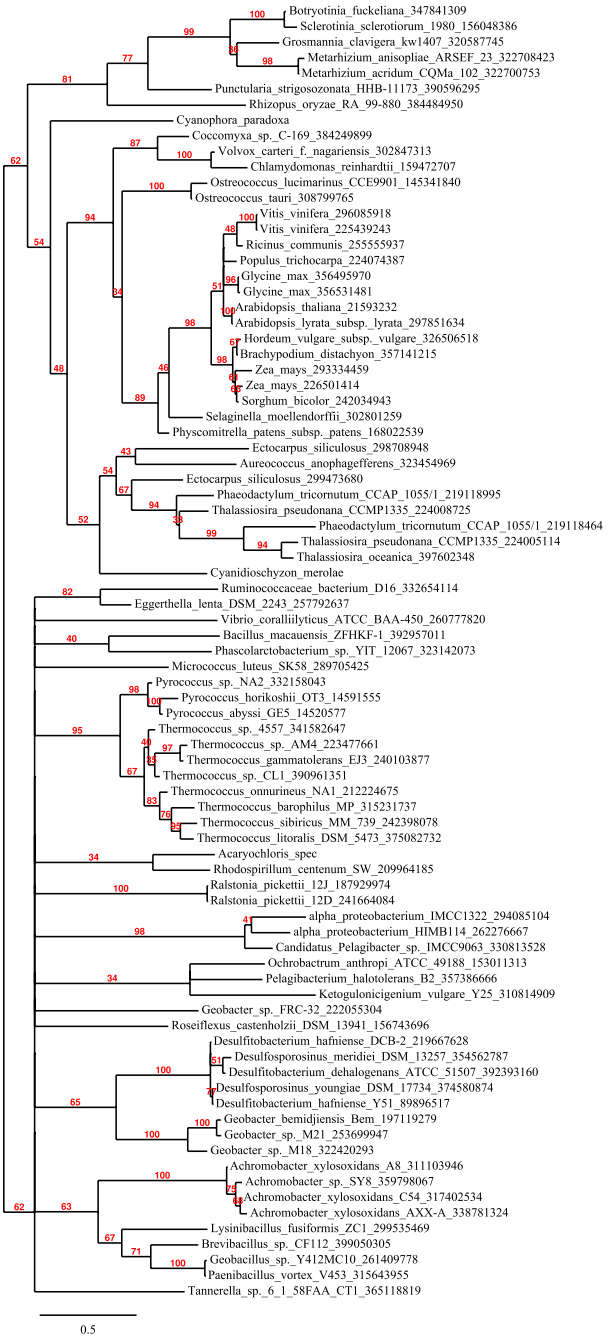

Fig. S6. Phylogenetic tree of PLGG1. AtPLGG1 was used as the query to Blast Explorer (www.phylogeny.fr/version2_cgi/one_task.cgi?task_type=blast), and the sequences suggested by the program were manually curated and fed to an "à la carte" phylogeny analysis (www.phylogeny.fr/version2_cgi/phylogeny.cgi) (1). Briefly, sequences were aligned with Muscle, and all positions with gaps were removed. The phylogenetic tree was calculated with PhyML and bootstrapped (100 repetitions). For display, all branches with <30% branch support were collapsed. The tree divides in two large branches, a bacterial and a eukaryotic branch. The sole cyanobacterium Acaryochloris spec is nested within the bacteria. In eukaryotes, the tree divides the fungi (more precisely the dikarya) from the archaeplastida. Within the archaeplastida, *Cyanophora paradoxa* separates from the red and green lineages, which themselves form separate branches. In the green lineage, the green algae separate from the streptophyta in which the moss branches before the fern. Monocots and dicots form separate branches. Because the fungi branch with the archaeplastida has a bootstrap support of 62%, the gene likely evolved before the archaeplastida and the fungi split, and it was lost from the other branches of life. Had the gene been acquired by a lateral gene transfer, one would expect it to branch within the bacteria. In higher plants, PLGG1 is nuclear encoded. For transport proteins of the chloroplasts, at least three different phylogenetic roots have been demonstrated: rooted in the Chlamydiae, rooted in the cyanobacteria and a host origin. PLGG1-like proteins do not appear in the Chlamydiae but in Cyanobacteria. The phylogenetic tree indicates that the gene is likely not acquired from the cyanobacteria because the single cyanobacterium PLGG1 is nested within the bacteria. Therefore, it is more likely that the cyanobacterium acquired it by lateral gene transfer from a bacterium. Hence, PLGG1 likely originated from the host.

1. Dereeper A, et al. (2008) Phylogeny.fr: Robust phylogenetic analysis for the non-specialist. *Nucleic Acids Res* 36(Web Server Issue):W465–W469.

Table S1. Rate of photosynthesis in WT and *plgg1-1* mutant plants

Plant genotype	High CO_2	Ambient CO_2		
	0 d	1 d	2 d	5 d
WT	14.56 ± 0.42	13.57 ± 0.46	13.42 ± 0.59	13.88 ± 0.40
plgg1	13.87 ± 0.23	7.01 ± 0.10	6.7 ± 0.76	4.62 ± 0.47

Photosynthetic rate was measured in high CO_2 (3000 ppm CO_2) at a light intensity of 150 μmol photons m^{-2} s^{-1} (0 d) and after shift to ambient CO_2 (380 ppm CO_2) after 1, 2, and 5 d. Values are mean of three biological replicates ± SD.

Table S2. Primers used for PCR amplification

Primer name	Sequence (5′–3′)
P1	CGTCGTCGTCTCCATACCCAT
P2	GTTTTGCCATAGGCTCGGCTT
P3	GCGTGGACCGCTTGCTGCAACT
P4	CACCATGGCTACTCTTTTAGCCACTCC
P5	GACACCTGAAGCAGCCGG
P6	TTCAATGTCCCTGCCATGTA
P7	TGAACAATCGATGGACCTGA
P8	CACCGGAGCATGAGTACCGTTACAATTG
P9	GACACCTGAAGCAGCCGG
P10	CACCGGAGCATGAGTACCGTTACAATTG
P11	ACTAACGGCCTTCGAGGAT
P12	CACCATGGCTACTCTTTTAGCCACTCC
P13	GACGACCGCTAGCAAACTCTG

All sequences are displayed in 5′–3′ orientation.

Table S3. Plants germinated and grown under different light regimens

Regimen	14 d		21 d	
	Size ratio WT/mutant	Percentage of mutant plants with lesions, %	Size ratio WT/mutant	Percentage of mutant plants with lesions, %
8-h L, 16-h D	1.58	50	1.94	60
16-h L, 8-h D	1.48	10	1.94	90
24-h L	1.36	nd	1.49	nd

Both the size difference compared with WT and the percentage of plants with lesions were scored. Although very young plants up to 2 wk of age benefit from extended light periods which alleviate the phenotype, plants from week three on suffer from extended light periods. D, dark; L, light; nd, not determined.